geothermal gradients within collisional orogens. Within the central Himalayas, the development of inverted field gradients, accompanied by substantial crustal melting, occurred at about 20 to 25 million years ago, about 25 to 35 My after the initiation of collision between India and Eurasia (*15*). Rocks currently at the surface were at depths of 20 to 40 km during regional metamorphism (*12*, *16*), yielding averaged rates of denudation of 1 to 2 km/My. Likewise, extensive tracts of lower (Indian) plate rocks with an exposed surface width greater than 300 km have been accreted episodically onto the upper (Eurasian) plate since the time of collision. Paleosubduction rates are unconstrained, but modern rates of convergence across the Himalayas are about 10 to 25 km/My (*17*). Radioactive heat production rates for metamorphic and igneous rocks of the Himalayas range from ~1.5 to >6 $\mu W/m^3$, with a significant proportion (>25%) of reported values in excess of 4 $\mu W/m^3$ (*18*). Thus, parameter values (especially $A = 3\ \mu W/m^3$) used to construct Fig. 2 are consistent with observations from the Himalayas. The agreement between timing, paleotemperatures and depths recorded in the central Himalayas, and the modeled thermal structure 32 My after collision (Fig. 2) suggests that redistribution of material with a high rate of heat production within the Himalayan orogen may have been an important factor in its thermal evolution.

Our model suggests that accretion and erosion and the attendant redistribution of HPE-enriched material exert first-order control on the thermal and metamorphic evolution of collisional orogens. Accretion leads to the development and maintenance of a wedge of HPE-enriched material within the upper plate of intracontinental subduction zones. Surface erosion also controls the geometry of this wedge and enhances heating within the upper plate by advecting material from deeper to shallower crustal levels.

REFERENCES AND NOTES

1. R. D. Hatcher Jr. *et al.*, in *The Appalachian-Ouachita Orogen in the United States*, R. D. Hatcher Jr., W. A. Thomas, G. W. Viele, Eds. (Geological Society of America, Boulder, CO, 1989), pp. 233–318; A. Ganser, *Geology of the Himalayas* (Wiley Interscience, London, 1964).
2. W. S. Pitcher, *Geol. Rundsch.* **76**, 51 (1987).
3. P. Le Fort, *Am. J. Sci.* **275A**, 1 (1975).
4. M. S. Hubbard, *J. Metamorph. Geol.* **7**, 19 (1989).
5. E. R. Oxburgh and D. L. Turcotte, *Schweiz. Mineral. Petrogr. Mitt.* **54**, 641 (1974).
6. P. C. England and A. Thompson, in *Collision Tectonics*, M. P. Coward and A. C. Ries, Eds. (Special Publication 19, Geological Society of America, Boulder, CO, 1986), pp. 83–94.
7. P. Bird, M. N. Toksoz, N. H. Sleep, *J. Geophys. Res.* **80**, 4405 (1975); Y. Shi and C. Y. Wang, *Geology* **15**, 1048 (1987); P. Karabinos and R. Ketcham, *J. Metamorph. Geol.* **6**, 559 (1988); C. Ruppel and K. V. Hodges, *Tectonics* **13**, 17 (1994).
8. C. Pinet and C. Jaupart, *Earth Planet. Sci. Lett.* **84**, 87 (1987).
9. F. A. Dahlen and T. D. Barr, *J. Geophys. Res.* **94**, 3906 (1989); T. D. Barr and F. A. Dahlen, *ibid.*, p. 3923; S. M. Peacock, in *Metamorphism and Crustal Evolution, Western Conterminous United States*, W. G. Ernst, Ed. (Prentice-Hall, Englewood Cliffs, NJ, 1987), pp. 953–975.
10. L. H. Royden, *J. Geophys. Res.* **98**, 4487 (1993).
11. K. V. Hodges, P. Le Fort, A. Pêcher, *Geology* **16**, 707 (1988).
12. A. Pêcher, *J. Metamorph. Geol.* **7**, 31 (1989).
13. M. Brunel and J. R. Kienast, *Can. J. Earth Sci.* **23**, 1117 (1986); M. P. Searle and A. J. Rex, *J. Metamorph. Geol.* **7**, 127 (1989).
14. P. Molnar and P. England, *J. Geophys. Res.* **95**, 4833 (1990); G. A. Houseman, D. P. McKenzie, P. Molnar, *ibid.* **86**, 6115 (1981).
15. M. S. Hubbard and T. M. Harrison, *Tectonics* **8**, 865 (1989); K. V. Hodges *et al.*, *Contrib. Mineral. Petrol.* **117**, 151 (1994); M. P. Searle, D. J. W. Cooper, A. J. Rex, in *Tectonic Evolution of the Himalayas and Tibet*, R. M. Shackleton, J. F. Dewey, B. F. Windley, Eds. (The Royal Society, London, 1988), pp. 117–150.
16. K. V. Hodges, M. S. Hubbard, D. S. Silverberg, *Philos. Trans. R. Soc. London Ser. A* **326**, 257 (1988).
17. H. Lyon-Caen and P. Molnar, *Tectonics* **4**, 513 (1985).
18. B. C. Scaillet, C. France-Lanord, P. Le Fort, *J. Volcanol. Geotherm. Res.* **44**, 163 (1990); P. Vidal, A. Cohcerie, P. Le Fort, *Geochim. Cosmochim. Acta*, **46**, 2279 (1982); A. M. Macfarlane, thesis, Massachusetts Institute of Technology (1992).

19. We thank two anonymous reviewers for helpful comments. Support was provided by NSF grant EAR 9418062 to K.V.H.

1 April 1996; accepted 12 June 1996

Lithologic Control of the Depth of Earthquakes in Southern California

Harold Magistrale* and Hua-wei Zhou

The depth distribution of southern California earthquakes indicates that areas underlain by schist basement rocks have a shallower (4 to 10 kilometers) maximum depth of earthquakes than do areas with other types of basement rocks. The predominant minerals in the schists become plastic at lower temperatures, and thus at shallower depths, than the minerals in the other basement rocks. The lateral variations in lithology will control the depth extent (and thus the magnitudes) of potential future earthquakes; these depths can be determined from the depth of the current background seismicity.

Earthquake magnitude is proportional to fault area. The fault area is the product of the length and the width of the fault on which brittle rupture occurs. Attempts to determine the magnitude of potential future earthquakes must therefore consider factors that influence the depth extent of rupture. Here we examine variations in the maximum depth of earthquakes in southern California and correlate a relatively shallow maximum depth to the presence of schist basement rocks.

The Late Cretaceous–early Tertiary Pelona, Orocopia, and Rand schists are structurally low rocks exposed in sparse outcrops (*1*) (Fig. 1). The schists are in low-angle fault contact with the overlying crystalline rocks (*1–5*). The emplacement mechanism of the mostly graywacke protolith is controversial: It is either in a west-dipping subduction zone under a continental fragment that was then accreted to western North America (*3*, *4*) or in an east-dipping subduction zone under the western North American margin (*5–7*). Subsequent faulting and uplift have exposed the schists. Seismic reflection surveys show that the schists extend over a large lateral area in the subsurface (*8–11*) and are >7 km thick (*12*). These surveys and the regional distribution of the schists (*1*, *3–7*) indicate that they probably underlay much of onshore southern California. Similarly, much of the inner continental borderland offshore of southern California is underlain by the Mesozoic Catalina Schist (*13–15*). This schist also has only sparse surface outcrop, but seismic reflection surveys and borehole samples indicate a widespread subsurface extent (*14*, *15*).

Recently, Zhou inverted southern California earthquake arrival times for crustal velocities and hypocenters (*16*). About 37,000 well-recorded earthquakes detected on the southern California seismic network (SCSN) between 1981 and 1994 provided data for the inversion (*17*). These earthquakes are representative of the more extensive SCSN earthquake catalog. We use the new hypocenters (Fig. 2) to examine variations in the hypocenter depths.

A major feature in the hypocenter depths is a 4- to 10-km change, or step, in the maximum depth of hypocenters. The step is particularly evident in the San Gorgonio Pass area (Fig. 2) as a result of the high density of hypocenters (*18*, *19*). The step can be traced as a regional feature that follows the San Andreas fault in the Coach-

H. Magistrale, Department of Geological Sciences, San Diego State University, San Diego, CA 92182, USA.
H.-w. Zhou, Department of Geosciences, University of Houston, Houston, TX 77204, USA.

*To whom correspondence should be addressed.

ella Valley and San Gorgonio Pass, continuing west and north along the San Gabriel fault to Tejon Pass (depths are shallower north and east of the faults) and then along the northwest side of the Tehachapi Mountains (depths are shallower to the southeast). In the Los Angeles basin, another step is identified along the Newport-Inglewood fault (depths are shallower to the west) and along the Malibu coast (depths are shallower to the south). In most places, the change in the maximum depth is <5 km wide, whereas along the Tehachapi Mountains, the southern Sierra Nevada, and the Malibu coast the change occurs gradually over zones tens of kilometers wide. The location of the step in the maximum depth of hypocenters (Fig. 2) is generally coincident with the edges of the schists in the subsurface (Fig. 1).

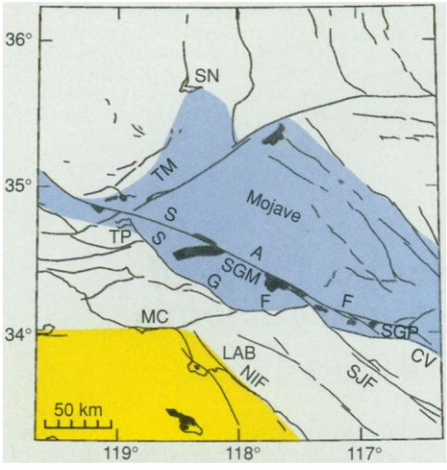

Fig. 1. Map of the southern California area showing the present-day surface exposures (*13, 30*) of schist rocks (black) and the subsurface extent (*31*) of the Catalina Schist (yellow) and the Pelona, Orcopia, and Rand schists (blue). Solid lines indicate the major faults and the coastline. Letters indicate the faults and places mentioned in the text. Abbreviations: CV, Coachella Valley; LAB, Los Angeles basin; MC, Malibu coast; NIF, Newport-Inglewood fault; SAF, San Andreas fault; SGF, San Gabriel fault; SGM, San Gabriel Mountains; SGP, San Gorgonio Pass; SJF, San Jacinto fault; SN, southern Sierra Nevada; TP, Tejon Pass; TM, Tehachapi Mountains.

The depth of earthquakes depends on four main factors: temperature, strain rate, fluid pressure, and rock composition (*20, 21*). Lateral variations in these factors will produce lateral variations in earthquake depths. We focus on rock composition to explain the change in the maximum depth of earthquakes because the change is abrupt, regional, and coincident with the edges of the schists.

The Pelona, Orocopia, Rand, and Catalina schists are composed predominantly of quartz and micas (*1, 13*). These minerals become plastic at much lower temperatures [≈300°C for quartz (*21*)] than minerals, such as feldspar [≈450°C (*21*)], that comprise the majority of the other types of basement rocks in southern California (6). In any geothermal gradient the schists will become plastic at a shallower depth than other basement rock types. Therefore, the schists will have a shallower maximum depth of brittle rupture (earthquakes) than the other basement rock types. For example (*18*), in the San Gorgonio Pass area, a reasonable geothermal gradient of 22°C km^{-1} and a surface temperature of 15°C results in a temperature of about 300°C at the 13-km maximum depth of seismicity seen north of the pass in an area underlain by Pelona Schist (*22*) and about 450°C at the 20-km maximum depth of seismicity in the mostly feldspar Peninsular Ranges type basement rocks (*23*) south of the pass, in agreement with the observed hypocentral depths (Fig. 2b, cross section A–A′). Thus, steps in the maximum hypocenter depths are produced where fault slip has juxtaposed the schists against other basement rock types near San Gorgonio Pass, along the San Gabriel fault (*22*), and along the Newport-Inglewood fault (*14*). More gradual slopes in the maximum hypocenter depths are produced where the crust has been warped by local uplift, such as in the Tehachapi Mountains (*11*) and the southern Sierra Nevada (*24*).

Schists abut other basement rocks along the San Andreas fault in the Coachella Valley (*22*) and along the offshore portion of the Newport-Inglewood fault (*14*). We therefore expect steps or slopes in the maximum hypocenter depths along those parts of the faults. Indeed, maximum hypocenter depths are shallower east of the San Andreas fault than west of the fault in Coachella Valley, and the maximum depths are shallower west of the offshore Newport-Inglewood fault than east of the fault. However, our seismicity data in those areas are too sparse to permit us to locate any steps with an accuracy of <20 km.

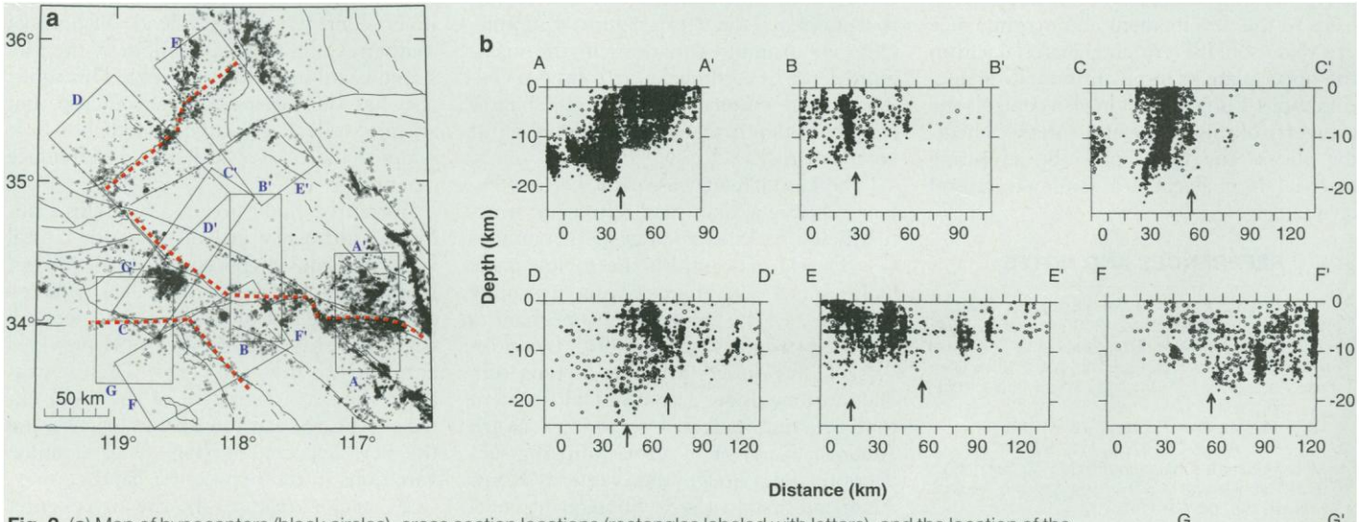

Fig. 2. (**a**) Map of hypocenters (black circles), cross section locations (rectangles labeled with letters), and the location of the steps in the hypocenter depths (red dashed lines). Where changes in the hypocenter depth occur as a gradual slope, the midpoint of the slope is plotted. The hypocenter symbols are scaled to earthquake magnitude. (**b**) Hypocenters plotted in cross section. The hypocenters within each rectangle in map view (a) are projected onto the cross section. The step is indicated by arrows. Where the hypocenter depth changes occur as a gradual slope (cross sections D–D′, E–E′, and G–G′), two arrows indicate the distance over which the depth change occurs. Vertical exaggeration, 3:1.

The step in the maximum earthquake depths provides a useful strain marker with which to measure the amount of slip on Quaternary faults. For example, the San Jacinto fault zone offsets the step by ≈20 km (Fig. 2a), which is compatible with an earlier measurement of the total slip measured farther south (25). Magistrale and Sanders recently used the apparent lack of offset in the step near the San Gorgonio Pass to argue for the accommodation of San Andreas fault zone slip by distributed deformation in that area (18).

The compositional control of the maximum depth of earthquakes can be used to estimate the depth extent of potential future earthquakes (26, 27). We compared the maximum depth defined by earthquakes before recent large earthquakes to the depth defined by the aftershock zones of the large earthquakes (Fig. 3). In every case, the maximum depth of rupture of the large earthquakes, as defined by the aftershock zones, was the same as the maximum depth of the earthquakes before the large earthquakes (28). Therefore, we conclude that the depth extent, and thus the magnitude, of potential future earthquakes in southern California can be determined from an examination of the depth of the background seismicity. This procedure may change estimates of the magnitudes of potential future earthquakes in the Los Angeles basin region (26) because steps in the maximum depth of the earthquakes run through and near that region (Fig. 2).

The accurate determination of the lateral variations in the thickness of the brittle crust should help to resolve the issue of whether the historic rate of earthquakes in the Los Angeles region is adequate to account for the geodetically determined strain rates (26, 29). If, as we have found, portions of the brittle crust are thinner than previously assumed, then more deformation would occur aseismically and less moment release would be required of the historic earthquakes.

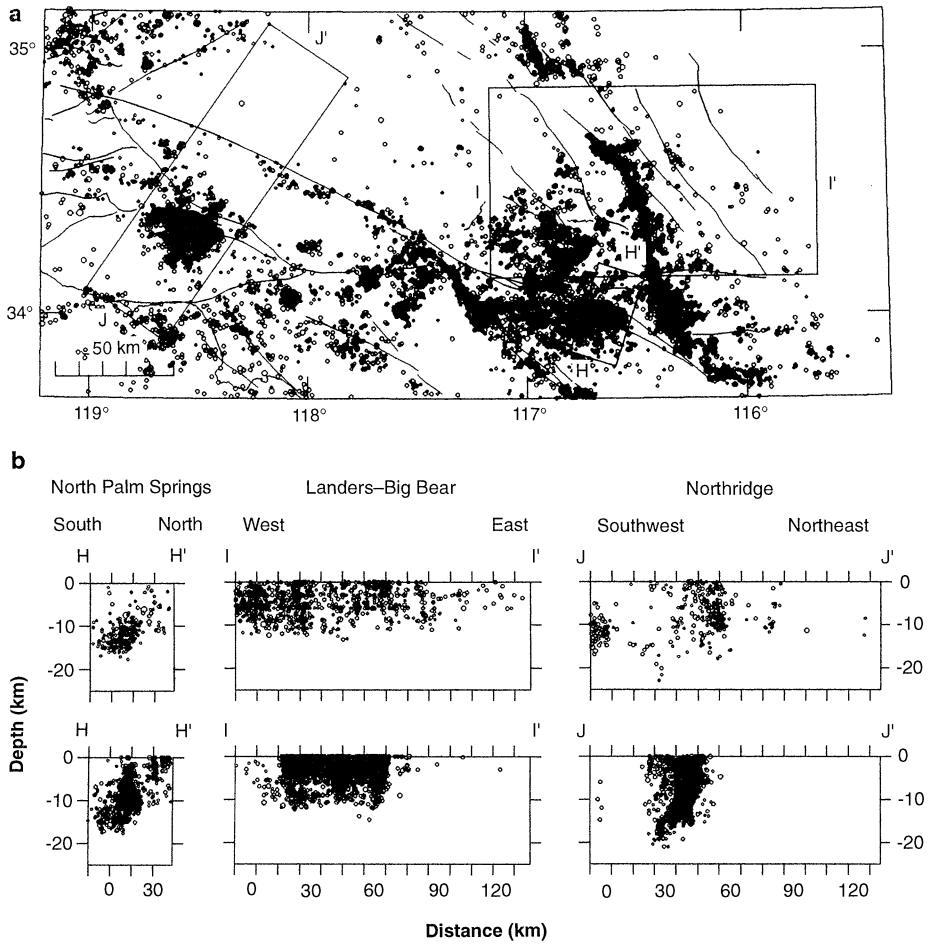

Fig. 3. (**a**) Map of hypocenters (black circles) and cross section locations (rectangles labeled with letters) across the aftershock zones of some larger earthquakes (1986 North Palm Springs, 1992 Landers–Big Bear, 1994 Northridge). Hypocenters of all dates are plotted. (**b**) Hypocenters plotted in cross section before (upper panels) and after (lower panels) the larger earthquakes. The background seismicity before the larger earthquakes defines the maximum depth of the aftershock zones (dense clouds of hypocenters). The Landers aftershocks, near 65 km in cross section I–I′, extend 1 to 2 km deeper than the background seismicity near 65 km but are generally no deeper than the background seismicity of the entire cross section. The background seismicity in cross section I–I′ is sparse, so we used a large cross section area to define a maximum depth. Vertical exaggeration, 2:1.

REFERENCES AND NOTES

1. G. Haxel and J. Dillon, in *Mesozoic Paleogeography of the Western United States*, D. Howell and K. McDougall, Eds. (Pacific Section Society of Economic Paleontologists and Mineralogists, Los Angeles, CA, 1978), pp. 453–470.
2. R. K. Dokka *et al.*, in *Geological Excursions in Southern California and Mexico*, M. J. Walawender and B. B. Hanan, Eds. (Department of Geological Sciences, San Diego State University, San Diego, CA, 1991), pp. 1–43.
3. P. L. Ehlig, in *The Geotectonic Development of California, Rubey Volume I*, W. G. Ernst, Ed. (Prentice-Hall, Englewood Cliffs, NJ, 1981), chap. 10.
4. J. T. Dillon, G. B. Haxel, R. M. Tosdal, *J. Geophys. Res.* **95**, 19953 (1990).
5. J. C. Crowell, in *The Geotectonic Development of California, Rubey Volume I*, W. G. Ernst, Ed. (Prentice-Hall, Englewood Cliffs, NJ, 1981), chap. 18.
6. W. Hamilton, in *Metamorphism and Crustal Evolution of the Western United States, Rubey Volume VII*, W. G. Ernst, Ed. (Prentice-Hall, Englewood Cliffs, NJ, 1988), chap. 1.
7. B. C. Burchfiel and G. A. Davis, in *The Geotectonic Development of California, Rubey Volume I*, W. G. Ernst, Ed. (Prentice-Hall, Englewood Cliffs, NJ, 1981), chap. 9.
8. M. J. Cheadle *et al.*, *Tectonics* **5**, 293 (1986); M. E. Spongberg and T. L. Henyey, *Geol. Soc. Am. Abstr. Programs* **19**, 454 (abstr.) (1987).
9. D. May *et al.*, *Eos* **63**, 1033 (abstr.) (1982).
10. R. S. Morris, thesis, San Diego State University (1990); ———, D. A. Okaya, E. G. Frost, P. E. Malin, *Geol. Soc. Am. Abstr. Programs* **18**, 160 (abstr.) (1986).
11. P. E. Malin *et al.*, *J. Geophys. Res.* **100**, 2069 (1995).
12. The thickness of the Pelona, Orocopia, and Rand schists seen in outcrop is up to about 4 km [summarized in (*30*)], but those outcrops are incomplete because the base of the schists is not anywhere exposed (*4*). Seismic reflection studies in the Mojave (*8*), San Gabriel Mountains (*9*), southeastern California (*10*), and Tehachapi Mountains (*11*) image the schists as a 7- to 15-km-thick layer. The top of the schists is near the surface around outcrops but elsewhere is typically 6 to 12 km deep (*8, 10, 11*). Marine seismic reflection studies image the Catalina Schist as at least 7 km thick (the base is not identified) with the top at a depth of 2 to 7 km (*14, 15*). Thus, the schists are at the same depth range as the step in the maximum depth of seismicity and are thick enough to contain the step. Where depth values were given in seismic two-way travel time, we converted to kilometers using a value of 6.5 km s^{-1} per second of two-way travel time, appropriate for schists at a depth of 10 km (*11*).
13. S. Sorensen, in *Metamorphism and Crustal Evolution of the Western United States, Rubey Volume VII*, W. G. Ernst, Ed. (Prentice-Hall, Englewood Cliffs, NJ, 1988), chap. 36; ———, G. E. Bebout, M. D. Barton, in *Geological Excursions in Southern California and Mexico*, M. J. Walawender and B. B. Hanan, Eds. (Department of Geological Sciences, San Diego State University, San Diego, CA, 1991), pp. 272–296; R. S. Yeats, *Am. Assoc. Pet. Geol. Bull.* **57**, 117 (1973).
14. D. G. Howell and J. Vedder, in *The Geotectonic Development of California, Rubey Volume I*, W. G. Ernst, Ed. (Prentice-Hall, Englewood Cliffs, NJ, 1981), chap. 16; J. G. Vedder, in *Geology and Resource Potential of the Continental Margin of Western North America and Adjacent Ocean Basins–Beaufort Sea to Baja California*, D. W. Scholl, A. Grantz, J. G. Vedder, Eds. (Circum-Pacific

Council for Energy and Minerals, Houston, TX, 1987), pp. 403–448.
15. J. K. Crouch and J. Suppe, *Geol. Soc. Am. Bull.* **105**, 1415 (1993).
16. H. Zhou, *J. Geophys. Res.* **99**, 15,439 (1994); *Eos* **75**, 483 (abstr.) (1994). This technique properly accounts for three-dimensional crustal and upper-mantle seismic velocity heterogeneities while determining hypocenters. The SCSN earthquake catalog hypocenters are found with a one-dimensional velocity model. However, the general features of the hypocenter depth patterns we discuss here are apparent in the best quality hypocenters in the SCSN earthquake catalog.
17. The earthquakes used here were selected to have small location errors as determined by the SCSN catalog and to have been recorded on at least 10 stations used for relocations. These selection parameters exclude earthquakes that are poorly constrained as a result of the low station density near the periphery of the SCSN. In the central part of the SCSN that we examine here, the hypocentral errors are <1 km (*16*).
18. H. Magistrale and C. Sanders, *J. Geophys. Res.* **101**, 3031 (1996).
19. S. M. Green, thesis, University of California, Los Angeles (1983); E. J. Corbett, thesis, California Institute of Technology (1984); T. H. Webb and H. Kanamori, *Bull. Seismol. Soc. Am.* **75**, 737 (1985); C. Nicholson, L. Seeber, P. Williams, L. R. Sykes, *J. Geophys. Res.* **91**, 4891 (1986); L. M. Jones, E. Hauksson, H. Qian, *Seismol. Res. Lett.* (abstr.) **64**, 22 (1993).
20. R. H. Sibson, *J. Geophys. Res.* **89**, 5791 (1984); R. Meissner and J. Strehlau, *Tectonics* **1**, 73 (1982); S. T. Tse and J. R. Rice, *J. Geophys. Res.* **91**, 9452 (1986); C. H. Scholz, *The Mechanics of Earthquakes and Faulting* (Cambridge Univ. Press, New York, 1990).
21. R. H. Sibson, *Bull. Seismol. Soc. Am.* **72**, 151 (1982).
22. J. C. Matti, D. M. Morton, B. F. Cox, *U.S. Geol. Surv. Open-File Rep. 85-355* (1985).
23. E. S. Larsen, *Geol. Soc. Am. Mem. 29* (1948).
24. D. A. Pickett and J. B. Saleeby, *J. Geophys. Res.* **98**, 609 (1993).
25. R. V. Sharp, *Geol. Soc. Am. Bull.* **78**, 705 (1967).
26. J. Dolan *et al.*, *Science* **267**, 199 (1995).
27. Working Group on California Earthquake Probabilities, *Bull. Seismol. Soc. Am.* **85**, 379 (1995).
28. In addition to the events shown in Fig. 3, we also checked the magnitude (*M*) 6.0 1987 Whittier Narrows, *M* 5.0 1988 Pasadena, *M* 5.0 1989 Malibu, *M* 4.6 1988 and *M* 5.2 1990 Upland, *M* 5.6 1991 Sierra Madre, and *M* 6.1 1992 Joshua Tree earthquakes. Some of these earthquakes occurred in areas underlain by schists and some in areas underlain by other kinds of rock; in every case the main shock–aftershock sequence had the same maximum depth as the local background seismicity. In some cases (for example, the Landers area in Fig. 3) the background seismicity was sparse but adequately defined the maximum depth.
29. C. M. Schiffries and T. L. Henyey, *Geotimes* **39**, 4 (1994); D. D. Jackson, *Seismol. Res. Lett.* **67**, 3 (1996).
30. C. E. Jacobson, *J. Geophys. Res.* **95**, 509 (1990).
31. To map the subsurface distribution of the Pelona, Orocopia, and Rand schists, we accept the conclusion of (*1*) that continuous schist is present under the western Mojave. Models of the emplacement of the schist protoliths also imply regional continuity of the schists (*1–7*), and seismic reflection surveys image the schists as continuous features extending beyond the survey areas (*8–11*). Constraints in the area of cross section A–A′ (Fig. 2) are from (*1, 7, 22*); cross section B–B′, from (*3, 32*); cross section C–C′, from (*3, 9, 32*); cross section D–D′, from (*11, 24*); and cross section E–E′, from L. T. Silver and J. A. Nourse, *Geol. Soc. Am. Abstr. Programs* **18**, 185 (abstr.) (1986); J. B. Saleeby, L. T. Silver, D. J. Wood, P. E. Malin, *ibid.* **25**, 141 (abstr.) (1993); and L. T. Silver, *ibid.* p. 147 (abstr.). Also, the southern Sierra Nevada Mountains are structurally continuous with the Tehachapi Mountains [J. B. Saleeby, D. B. Sams, R. K. Kistler, *J. Geophys. Res.* **92**, 10,443 (1987)] where schist is present (*11, 24*). The subsurface distribution of the Catalina schist is from (*13–15*); T. L. Wright, in *Active Margin Basins, Am. Assoc. Pet. Geol. Mem. 52*, K. T. Biddle, Ed. (American Association of Petroleum Geologists, Tulsa, OK, 1991), pp. 35–134; and J. E. Schoellhamer and A. O. Woodford, *U.S. Geol. Surv. Oil Gas Invest. Map OM-117* (1951). There is minor disagreement about the eastern limit of the Catalina Schist under part of the Los Angeles basin (*14, 15*); here we follow (*14*).
32. A. P. Barth, C. E. Jacobson, D. J. May, in *Geological Excursions in Southern California and Mexico*, M. J. Walawender and B. B. Hanan, Eds. (Department of Geological Sciences, San Diego State University, San Diego, CA, 1991), pp. 186–198.
33. We thank L. Silver for providing a compilation of the subsurface distribution of the schists; C. Sanders for clarifying ideas; and S. Day, E. Frost, and G. Girty for reviews of the manuscript. Supported in part by NSF grant EAR-9218704 to H.Z.

26 February 1996; accepted 29 May 1996

Mechanism of Phreatic Eruptions at Aso Volcano Inferred from Near-Field Broadband Seismic Observations

Satoshi Kaneshima,* Hitoshi Kawakatsu,† Hirotoshi Matsubayashi, Yasuaki Sudo, Tomoki Tsutsui, Takao Ohminato, Hisao Ito, Koichi Uhira, Hitoshi Yamasato, Jun Oikawa, Minoru Takeo, Takashi Iidaka

Broadband seismometers deployed at Aso volcano in Japan have detected a hydrothermal reservoir 1 to 1.5 kilometers beneath the crater that is continually resonating with periods as long as 15 seconds. When phreatic eruptions are observed, broadband seismograms elucidate a dynamic interplay between the reservoir and discharging flow along the conduit: gradual pressurization and long-period (~20 seconds) pulsations of the reservoir during the 100 to 200 seconds before the initiation of the discharge, followed by gradual deflation of the reservoir concurrent with the discharging flow. The hydrothermal reservoir, where water and heat from the deeper magma chamber probably interact, appears to help control the surface activity at Aso volcano.

The activity of volcanoes has been conventionally monitored with short-period seismometers (>1 Hz) (*1*) and with geodetic instruments including strain- and tilt-meters (*2*). Short-period records of volcanic earthquakes and tremors describe stress accumulation around magma chambers or fluid flow through conduits, whereas strain- and tilt-meters mainly record quasi-static deformation associated with slower responses of pressure sources, such as a magma chamber. Ground motions in the frequency range from 0.01 to 1 Hz, which has not been widely monitored, may elucidate the detailed structure of pressure sources and the dynamics of mass advection during an eruption (*3*).

S. Kaneshima, Department of Earth and Planetary Physics, Faculty of Science, University of Tokyo, Bunkyo-ku, Tokyo 113, Japan.
H. Kawakatsu, H. Matsubayashi, J. Oikawa, M. Takeo, T. Iidaka, Earthquake Research Institute, University of Tokyo, Bunkyo-ku, Tokyo 113 Japan.
Y. Sudo and T. Tsutsui, Aso Volcanological Laboratory, Faculty of Science, Kyoto University, Aso, Kumamoto 869-14, Japan.
T. Ohminato and H. Ito, Geological Survey of Japan, Tsukuba, Ibaraki 305, Japan.
K. Uhira, Japan Meteorological Agency, Chiyoda-ku, Tokyo 110, Japan.
H. Yamasato, Meteorological Research Institute, Tsukuba, Ibaraki 305, Japan.

*Currently on leave at Department of Geology, University of Bristol, Bristol BS8 1RJ, UK.
†To whom correspondence should be addressed. E-mail: hitoshi@eri.u-tokyo.ac.jp

From April 1994 through March 1995, we operated 10 to 12 broadband, three-component velocity seismometers around Aso volcano in Japan (Fig. 1) (*4*). When Aso volcano was quiescent, that is, when there was a lack of major surface activity at the crater, our seismometers detected tremors with unusually long periods (~15 s) (*5, 6*) almost continuously throughout the 1 year of the experiment. A long-period tremor (LPT) consisted of a series of isolated wave packets with an amplitude of about 1 μm with a duration of about 30 s (Fig. 2). Amplitude spectra at three stations obtained by stacking many events showed that the dominant period of each LPT was about 15 s (Fig. 3). The observed spectra also showed other consistent long-period peaks at about 7.5, 5, and 3 s, which correspond to the second, third, and fifth overtones of the harmonic oscillation with a fundamental period of 15 s (Fig. 3). The presence of overtones indicates that the LPT was an oscillation of a resonator (*7*).

At most stations near the crater, the horizontal particle motions of LPTs in the 10- to 30-s bandpassed seismograms were rectilinear and pointed toward the crater. The particle motions in the radial plane showed that the incident angles of the LPTs observed at most stations around the crater ranged from about 35° to 70° (Fig. 4B). Assuming that